Study on the Occurrence of Parametric Roll in Bichromatic Waves

Tae-Young Kim, Yonghwan Kim, Dong-Min Park
Department of Naval Architecture and Ocean Engineering, Seoul National University
Seoul, Korea

Introduction

The dynamic stability of ship in waves has been of interest for many years. Small or mid-size ships such as fishing vessels can be danger due to broaching and surf-riding, while the larger commercial ships can be damaged due to parametric rolling. There are more engineering issues for combatants, and damaged stability is also one of recent big concerns. Recently IMO tries to create a regulation for the dynamic stability of ships.

This study considers parametric roll, one of the ship dynamic problems, which is important for the design and operation of some commercial ships such as containerships, cruise ships, and Ro-Ro ships. The mathematical definition of 'parametric' indicates self-excitation or parametric excitation which can be explained in the form of the Mathieu equation. Many researches proved the possibility of the occurrence of very large roll angle in head or following waves when the wave encounter frequency is twice that of the roll natural frequency. According to previous studies, the analysis of parametric roll requires taking into account the actual wetted ship surface in motion analysis. Some researchers approximated the nonlinear restoring force by using harmonic variation of metacentric height, $\overline{GM}$, then such approximation leads the classical equation of motion to the Mathieu equation(e.g. Pauling and Rosenberg, 1959, Nayfeh,1988). Numerical computations have been also used to simulate the parametric roll occurrence. For instant, France et al. (2003) and Shin et al. (2004) introduced the computational results obtained by using Rankine panel method, and Spanos and Papanikolaou (2007) applied an impulse-response-function (IRF) method for parametric roll.

In this study, we introduce the difference-frequency-induced parametric roll which hasn't been introduced in previous researches. The existence of the difference-frequency-induced parametric roll is proved by using theoretical, numerical, and experimental studies. By using the Mathieu equation for bichromatic excitation, it can be shown that the difference-frequency-induced parametric roll is a kind of the second-order resonance of roll motion. In numerical study, both Rankine panel and IRF methods are applied for simulating the parametric roll in bichromatic waves. The experimental observation is also introduced for a cruise ship, showing the occurrence of large roll motion in bichromatic-wave conditions.

Theoretical Background

Let us consider a ship moving with a steady speed $\vec{U}$. The occurrence of parametric roll can be easily predicted by using the resonance analysis which includes the second-order property of wetted surface variation. Like previous study, a simple approximation of metacentric height of the ship in two harmonic waves with encounter frequencies $\omega_{e,a}$ and $\omega_{e,b}$ can be approximated as follows:

$$\overline{GM} = \overline{GM}_{mean} + \overline{GM}_a \cos\left(\omega_{e,a} t\right) + \overline{GM}_b \cos\left(\omega_{e,b} t + \alpha\right) \tag{1}$$

where $\overline{GM}_{mean}$ is the average of metacentric height, i.e. $\left(\overline{GM}_{max} + \overline{GM}_{min}\right)/2$, and $\overline{GM}_a$ and $\overline{GM}_b$ are the variation amplitude of the two wave components. In addition, α is a phase difference of the two wave components. Then the undamped 1-DOF equation of roll motion can be written as

$$\ddot{\varphi} + \left\{\Omega_n^2 + \Omega_a^2 \cos\left(\omega_{e,a} t\right) + \Omega_b^2 \cos\left(\omega_{e,b} t + \alpha\right)\right\}\varphi = \tilde{M}(\omega_{e,a}, \omega_{e,b}; t) \tag{2}$$

where

$$\Omega_n^2 = \Delta\overline{GM}_{mean} / \left(I_{44} + I_{44,ab}\right) \text{ and } \Omega_a^2 = \Delta\overline{GM}_a / \left(I_{44} + I_{44,ab}\right), \quad \Omega_b^2 = \Delta\overline{GM}_b / \left(I_{44} + I_{44,ab}\right) \tag{3}$$

where φ is roll angle which and $\tilde{M}(\omega_{e,a}, \omega_{e,b}; t)$ refers to the roll moment normalized by the mass and added mass moment of inertia. Here, Δ and I_{44} are the ship mass and the mass moment of inertia. $I_{44,ab}$ indicates the representative added moment of inertia for the two frequencies. It should be noted that there may be some differences between $I_{44,ab}$ and the added moment of inertia for the two frequencies. However, it is assumed that the differences are relatively small, so that Eq.(3) can be the leading-order equation of roll.

The stability of roll motion can be checked by observing the homogeneous equation of Eq.(2). By using a non-dimensional time scale parameter, $\tau = \omega_{e,a} t$, introduced to one frequency component, the homogeneous equation of Eq.(2) can be written as

$$\frac{d^2\varphi}{d\tau^2} + \left\{\nu + \varepsilon\cos(\tau) + \varepsilon\mu\cos\left(1 + \varepsilon\Lambda\right)\tau\right\}\varphi = 0 \tag{4}$$

where $\nu = \Omega_n^2 / \omega_{e,a}^2$, $\varepsilon = \Omega_a^2 / \omega_{e,a}^2$, $\mu = \Omega_b^2 / \Omega_a^2$ and $\Lambda = \left(\omega_{e,b} - \omega_{e,a}\right)\omega_{e,a} / \Omega_a^2$, respectively. Here, the phase difference, α, is ignored because the phase difference does not affect stability. Eq.(4) is an undamped quasi-periodic Mathieu equation. Rand et al. (2003) have verified the stability of the solution by application of a numerical integration and perturbation method. Two examples of the stability diagram are plotted in Fig. 1 by using the numerical method. Obtained diagrams were similar to the results of Rand et al. (2003). In this plots, the shaded area presents stable and bright unstable zones. Here, a parameter δ_1 is defined as $\nu = 1/4 + \varepsilon\delta_1$. This stability analysis implies the possibility of unstable roll motion in bichromatic waves. Such unstable roll can be another source of parametric roll.

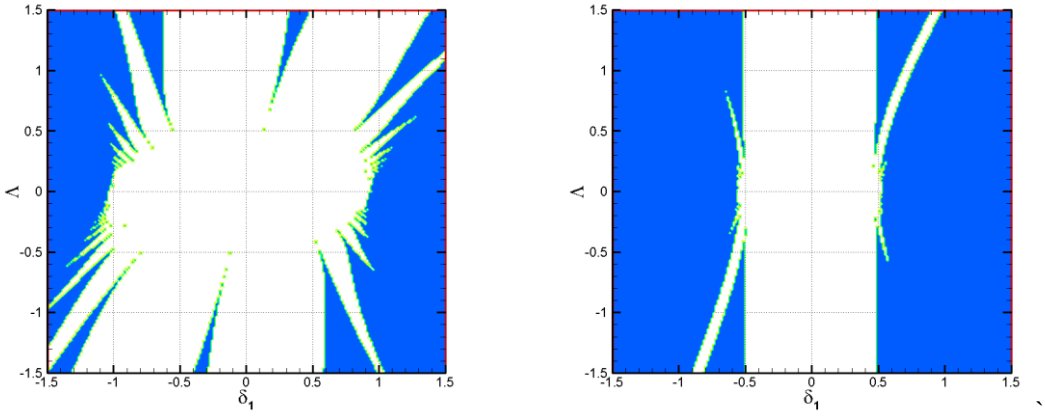

(a) $\varepsilon = 0.1, \mu = 1$ (b) $\varepsilon = 0.1, \mu = 0.1$

Fig. 1 Two example of stability diagram for quasi-periodic Mathieu equation (shaded: stable, bright: unstable)

Numerical Method

To observe the occurrence of parametric roll in bichromatic waves, two different numerical methods are applied: impulse-response function(IRF) approach and Rankine panel method. Particularly, the both methods are based on weakly nonlinear formulation which is a mixture of linear hydrodynamic force and nonlinear Froude-Krylov and restoring force. In the IRF approach, the equation of motion including the nonlinear Froude-Krylov and restoring forces is written as follows:

$$\begin{aligned}&(M + M_\infty)\ddot{\xi} + \int_0^t R(t-\tau)\dot{\xi}(\tau)d\tau \\ &\quad = (F_{F.K.})_{nonlinear} + (F_{Rest})_{nonlinear} + F_{Diff} + F_{viscous} + F_{external}\end{aligned} \tag{5}$$

where the force terms can consist of nonlinear Froude-Krylov and restoring forces, linear diffraction force, viscous force, and external forces. The diffraction force can be converted from the frequency-domain solution, and viscous force is added to the roll component. In this study, an equivalent linear damping mechanism is applied. The external force includes the soft spring mechanism for non-restoring motions, but no such external force is needed for roll motion.

In the case of Rankine panel method, the present computation was carried out by using WISH (computer program for Wave-Induced nonlinear Ship motion and structural loads, Kim et al., 2007). In this method, the total velocity potential is decomposed into three components as follows:

$$\phi(\vec{x},t) = \Phi(\vec{x},t) + \phi_I(\vec{x},t) + \phi_d(\vec{x},t) \tag{6}$$

where Φ, ϕ_I, ϕ_d are the basis flow, incident wave, and disturbance velocity potentials, respectively. This program adopts the bi-quadratic B-spline basis function for physical variables, so that the variables can be written as follows:

$$\left[\phi_d \quad \frac{\partial\phi_d}{\partial n} \quad \zeta_d\right]^T(\vec{x},t) = \sum_j \left[(\phi_d)_j \quad \left(\frac{\partial\phi_d}{\partial n}\right)_j \quad (\zeta_d)_j\right]^T(t)B_j(\vec{x}) \tag{7}$$

where $B_j(\vec{x})$ is the B-spline basis function. By solving the Green second identity as well as the above boundary conditions, the solution of the boundary value problem can be obtained.

$$\phi_d + \iint_{S_B} \phi_d \frac{\partial G}{\partial n} dS - \iint_{S_F} \frac{\partial\phi_d}{\partial n} G dS = \iint_{S_B} \frac{\partial\phi_d}{\partial n} G dS - \iint_{S_F} \phi_d \frac{\partial G}{\partial n} dS \tag{8}$$

The amplitude of roll angle is sensitive to the viscous effect. In this computation, the equivalent damping coefficient is defined as follows is applied for the viscous force.

$$F_{viscous} = -b_{equi\_viscous}\dot{\xi} = -\left(b + 2\gamma\sqrt{(M + M_\infty)C}\right)\dot{\xi} \tag{9}$$

b is the wave damping coefficient and γ means the ratio with respect to the critical damping coefficient. In addition, C refers to the restoring coefficient of roll motion.

Computational Results

Two ships, a large containership and a cruise ship, are considered for numerical computation, since these types of ships have a higher possibility of parametric roll in ocean waves than other types of ship. Table 1 shows the principal dimensions of the two ships, and Fig.2 shows the example of solution grids and instantaneous wave contour around the cruise ship.

Table 1. Principal dimensions of test ship model

Parameters	Container	Cruise
LBP (m)	286.3	242
Beam (m)	40.3	36
Draft (m)	13.127	8.39
$\overline{GM}$ (m)	1.14	2.34
Displacement (m^3)	92,952	49,756
Natural frequency ($\omega_n\sqrt{L/g}$)	1.10	1.49

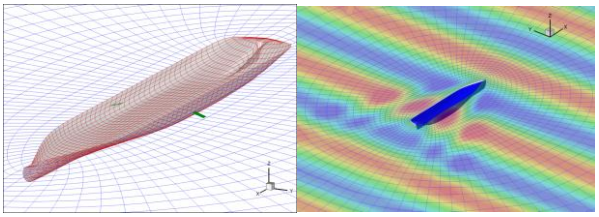

Fig. 2 Examples of solution grids and instantaneous wave contours for the cruise ship: Fn=0.211, β=180˚, $\omega_e\sqrt{L/g}$ =3.10

Fig. 3 shows the linear and nonlinear roll motions of 10,000 TEU containership in single and two wave components. When the ship is under the single-wave excitation at the frequency of either $\omega_e\sqrt{L/g} = 2.88$ or 4.13, both the linear and nonlinear roll motions are very small and regular without any significant development of large roll motion. However, when the two waves are imposed at the same time, i.e. in the case of bichromatic waves, the linear and nonlinear roll motions significantly differ. In particular, the nonlinear solution shows very large roll motion which must be generated by the high-order nonlinear effect. Fig. 3 implies much stronger nonlinear effect on roll motion in weaker wave excitation. Fig. 4 shows the Frourier components of the nonlinear restoring and FK moments in the bichromatic wave case of Fig.3. From Fig.4, it is obvious that the nonlinear restoring plays a key role in nonlinear roll.

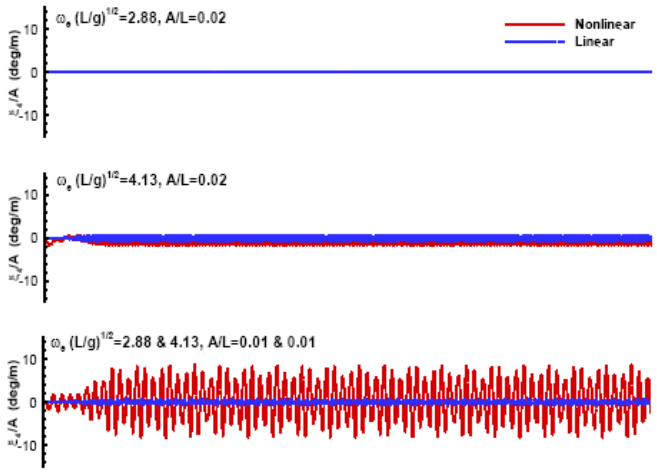

Fig. 3 Linear and nonlinear motions in the single and binchromatic waves: Fn=0.049, β=120˚, $\omega_e\sqrt{L/g} = 2.88$ and $\omega_e\sqrt{L/g} = 4.13$

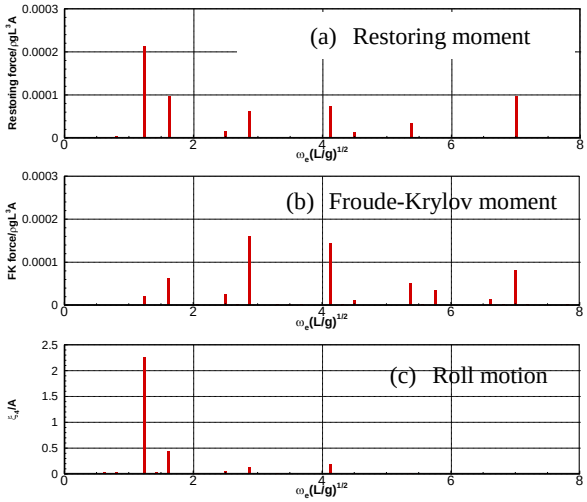

(c) Roll motion

Fig. 4 Fourier components of nonlinear signals in a bichromatic wave case: Fn=0.049, β=120˚, $\omega_e\sqrt{L/g} = 2.88$ and $\omega_e\sqrt{L/g} = 4.13$, A/L=0.01 for each component

As shown in Fig. 4, the nonlinear restoring moment has a stronger effect at a low frequency of around 1.25 than that at the linear wave frequencies, which is believed to be due to the difference-frequency effect of the two wave components. It should be mentioned that the nonlinear signals in these figures are the total nonlinear values which include the linear component. Therefore, the Fourier components consist of the linear components at the normalized frequencies of 2.88 and 4.13, and the four second-order components at the frequencies of 5.76(2x2.88), 8.26(2x4.13), 1.25(4.13-2.88), and 7.01(4.13+2.88), and the higher-order components. All of these

appear in Fig. 4(a), except for the component of 8.26 which is in the out of frequency range.

This result may be somewhat surprising, since the second-order component is generally much less than the linear components. However, in this case, the large second-order component must be due to the large roll motion at frequency 1.25, which is near the roll natural frequency. This explains that the difference-frequency effect triggers the unstable roll motion.

The occurrence of parametric roll in bichromatic waves can also be observed in the cruise ship. Fig. 5 shows the time-histories of nonlinear roll motions in the single and bichromatic waves. Similarly to the container ship, the roll motion in the bichromatic waves is much larger than the linear solution as well as the summation of the two roll motions of single components. Furthermore, the difference-frequency-induced parametric roll is obvious.

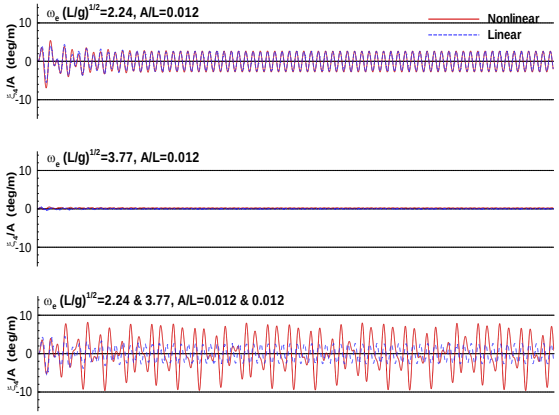

Fig. 5 Linear and nonlinear motions in the single and bichromatic waves: Fn=0.053, β=120˚, $\omega_e\sqrt{L/g}$ =2.24, 3.7

Experimental Validation

A set of model tests for the cruise ship has been carried out at the ocean basin of Ulsan University, and the model scale was 1/100. This experiment has been focused on global motion, not specifically on parametric rolling. However, a series of test have been carried out to observe the occurrence of parametric roll in bichromatic waves (Kim & Kim 2010). Fig. 6 shows the measured wave elevation, the Fourier component of measured waves, and the snapshots of ship rolling for a bichromatic wave condition. Although the same amplitude of the two components was expected, it did not occur in the actual experiment. However, the occurrence of parametric rolling in the bichromatic wave is obvious.

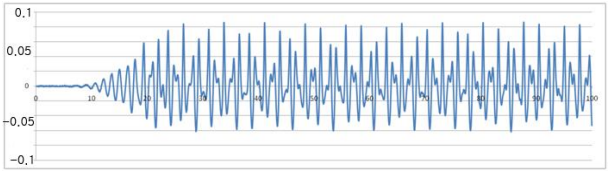

(a) Measured wave elevation

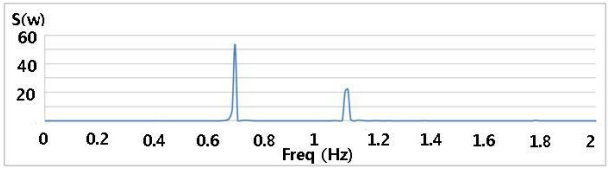

(b) Fourier components of wave elevation

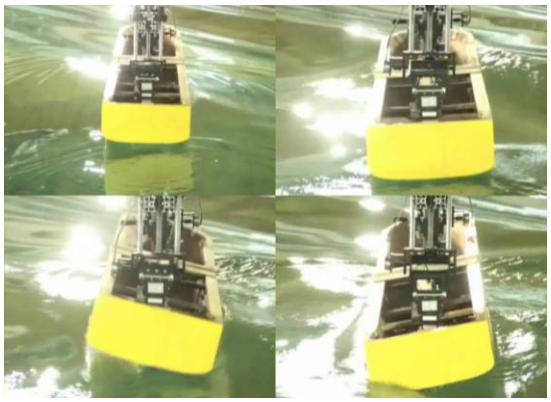

(c) Snapshots of parametric roll occurrence

Fig. 6 Experiment of difference-frequency-induced parametric roll for Cruise ship: Fn=0.053, β=120˚, $\omega_e\sqrt{L/g}=2.24$ and $\omega_e\sqrt{L/g}=3.77$, A/L=0.012 each component

References

France, W.M., Levadou, M., Treakle, T.W., Paulling, J.R., Michel, K. and Moore, C. (2003). "An Investigation of Head-Sea Parametric Rolling and its Influence on Container Lashing Systems," *Marine Technology*, Vol 40, No 1, pp 1-19.

Kim, K.H., Kim, Y. and Kim, Y. (2007). WISH JIP project and manual, Marine Hydrodynamics Laboratory, Seoul National Univeristy.

Kim, Y. and Kim, J.H. (2010). Analysis of nonlinear seakeeping, motion control, and comfort analysis on Daewoo cruise ship, Project report and user's manual for DSME-CRUISE, Marine Hydrodynamic Laboratory, Seoul National University.

Nayfeh, A.H. (1988). "On the undesirable roll characteristics of ships in regular seas," *Journal of Ship Research*, Vol 32, No 2, pp 89-103.

Paulling, J.R. and Rosenberg, R.M. (1959). "On unstable ship motions resulting from nonlinear coupling," *Journal of Ship Research*, Vol 3, No 1, pp 36-46.

Rand, R., Guennoun, K. and Belhaq, M. (2003). "2:2:1 Resonance in the Quasiperiodic Mathieu Equation," *Nonlinear Dynamics*, Vol. 31, No. 4, pp 367-374.

Shin, Y.S., Belenky, V.L, Pauling, J.R., Weems, K.M. and Lin W.M. (2004). "Criteria for parametric roll of large container ships in longitudinal seas," *SNAME Annual Meeting*, Washington DC.

Spanos, D. and Papanikolaou, A. (2007). "Numerical simulation of parametric roll in head seas," *International Shipbuilding Progress*, 54, pp 249-267.